frequency. By comparison, the r.m.s. (root mean square) displacement x_m of the C_{60} molecule in the mth vibrational level is given by $x_m = (2m+1)^{1/2}x_0$, where $x_0 = (hf/k)^{1/2} \approx 3\,\mathrm{pm}$. Although the exact values of these simple estimates change when the second metal electrode is included in the model, the qualitative conclusions of the model remain essentially the same. The present estimates pertain to the situation where the coupling between C_{60} and two electrodes is strongly asymmetric.

The C_{60}–surface vibration discussed above can account for the 5-meV conductance features in a unifying fashion. The first $\partial I/\partial V$ peak at the boundary of the conductance-gap region is observed when an electron hops on or off C_{60} with the system staying in the ground vibrational level. Additional $\partial I/\partial V$ peaks on the $V_g < V_c$ side appear when an electron hops onto C_{60}^{n-} to generate $C_{60}^{(n+1)-}$ in excited vibrational states. The $\partial I/\partial V$ peaks on the $V_g > V_c$ side signify, on the other hand, an event where an electron hops off $C_{60}^{(n+1)-}$, leaving C_{60}^{n-} in excited vibrational levels. Multiple $\partial I/\partial V$ peaks on the same side of V_c indicate that multiple vibrational quanta are excited.

This process is thus reminiscent of the Franck–Condon processes encountered in electron-transfer and light-absorption processes in molecules, where the vibrational excitation accompanies the electronic motion[24]. Within the harmonic approximation, the vibrational matrix elements for these processes can readily be calculated, and the ratio δ/x_0 determines the number of vibrational quanta typically excited by the tunnelling electron. According to the estimates discussed above, $\delta/x_0 \approx 1$ in a single-C_{60} transistor. The number of $\partial I/\partial V$ peaks visible in Fig. 2 in general confirms this expectation as only a few $\partial I/\partial V$ peaks are observed in most devices.

One device that does not follow this general trend is the one shown in Fig. 2d. As described previously, this device exhibits many $\partial I/\partial V$ peaks on both sides of V_c. In addition, the peak intensities do not show the simple variations expected from the single-mode Franck–Condon situation[24]. The anomalous behaviour may be related to the highly asymmetric coupling of C_{60} and the two electrodes in this particular device. This asymmetry is demonstrated by the different slopes of the upward and downward $\partial I/\partial V$ lines in the V–V_g plane. The variations of peak intensities may be due to the presence of other degrees of freedom in the system, such as the C_{60} motion perpendicular to the surface normal.

Unexplained features exist in other devices as well. In the data in Fig. 2a, a small (≤ 1 meV) energy splitting is observed for many of the lines. This splitting may arise from the C_{60} centre-of-mass motion perpendicular to the surface normal discussed above. Unfortunately, the nature of the potential for this motion is not known, owing to the lack of detailed knowledge of the electrode geometry near C_{60}, and quantitative support of this assignment is thus lacking at present.

The transport measurements presented here demonstrate that single-electron-tunnelling events can be used both to excite and probe the motion of a molecule: indeed, the single-C_{60} transistor behaves as a high-frequency nanomechanical oscillator. Furthermore, the oscillations of the C_{60} molecule must be treated in a quantized fashion, showing that this is a true quantum 'mechanical' system. We expect that the coupling between the quantized electronic and mechanical degrees of freedom will be generically important in electron transport through nanomolecular systems[25,26]. □

Received 17 March; accepted 30 June 2000.

1. Grabert, H. & Devoret, M. H. *Single Charge Tunneling* (Plenum, New York, 1992).
2. Sohn, L. L., Kouwenhoven, L. P. & Schön, G. *Mesoscopic Electron Transport* (Kluwer Academic, Dordrecht, 1997).
3. Bumm, L. A. *et al.* Are single molecular wires conducting? *Science* **271,** 1705–1707 (1996).
4. Reed, M. A., Zhou, C., Muller, C. J., Burgin, T. P. & Tour, J. M. Conductance of a molecular junction. *Science* **278,** 252–254 (1997).
5. Datta, S. *et al.* Current-voltage characteristics of self-assembled monolayers by scanning tunneling microscopy. *Phys. Rev. Lett.* **79,** 2530–2533 (1997).
6. Porath, D., Levi, Y., Tarabiah, M. & Millo, O. Tunneling spectroscopy of isolated C_{60} molecules in the presence of charging effects. *Phys. Rev. B* **56,** 9829–9833 (1997).
7. Joachim, C. & Gimzewski, J. K. An electromechanical amplifier using a single molecule. *Chem. Phys. Lett.* **265,** 353–357 (1997).
8. Stipe, B. C., Rezaei, M. A. & Ho, W. Single-molecule vibrational spectroscopy and microscopy. *Science* **280,** 1732–1735 (1998).
9. Klein, D. L., McEuen, P. L., Bowen Katari, J. E., Roth, R. & Alivisatos, A. P. An approach to electrical studies of single nanocrystals. *Appl. Phys. Lett.* **68,** 2574–2576 (1996).
10. Klein, D. L., Roth, R., Lim, A. K. L., Alivisatos, A. P. & McEuen, P. L. A single-electron transistor made from a cadmium selenide nanocrystal. *Nature* **389,** 699–701 (1997).
11. Park, H., Lim, A. K. L., Park, J., Alivisatos, A. P. & McEuen, P. L. Fabrication of metallic electrodes with nanometer separation by electromigration. *Appl. Phys. Lett.* **75,** 301–303 (1999).
12. Banin, U., Cao, Y., Katz, D. & Millo, O. Identification of atomic-like electronic states in indium arsenide nanocrystal quantum dots. *Nature* **400,** 542–544 (1999).
13. Kim, S.-H., Medeiros-Ribeiro, G., Ohlberg, D. A. A., Williams, R. S. & Heath, J. R. Individual and collective electronic properties of Ag nanocrystals. *J. Phys. Chem. B* **103,** 10341–10347 (1999).
14. Bockrath, M. *et al.* Single-electron transport in ropes of carbon nanotubes. *Science* **275,** 1922–1925 (1997).
15. Tans, S. J. *et al.* Individual single-wall carbon nanotubes as quantum wires. *Nature* **386,** 474–477 (1997).
16. Tans, S. J., Verschueren, A. R. M. & Dekker, C. Room-temperature transistor based on a single carbon nanotube. *Nature* **393,** 49–52 (1998).
17. Bockrath, M. *et al.* Luttinger-liquid behaviour in carbon nanotubes. *Nature* **397,** 598–601 (1999).
18. Gorelik, L. Y. *et al.* Shuttle mechanism for charge transfer in Coulomb blockade nanostructures. *Phys. Rev. Lett.* **80,** 4526–4529 (1998).
19. Dresselhaus, M. S., Dresselhaus, G. & Eklund, P. C. *Science of Fullerenes and Carbon Nanotubes* (Academic, New York, 1996).
20. Green, W. H. Jr *et al.* Electronic structures and geometries of C_{60} anions via density functional calculations. *J. Phys. Chem.* **100,** 14892–14898 (1996).
21. Heid, R., Pintschovius, L. & Godard, J. M. Eigenvectors of internal vibrations of C_{60}: Theory and experiment. *Phys. Rev. B* **56,** 5925–5936 (1997).
22. Chavy, C., Joachim, C. & Altibelli, A. Interpretation of STM images: C_{60} on the gold (110) surface. *Chem. Phys. Lett.* **214,** 569–575 (1993).
23. Ruoff, R. S. & Hickman, A. P. Van der Waals binding of fullerenes to a graphite plane. *J. Phys. Chem.* **97,** 2494–2496 (1993).
24. Schatz, G. C. & Ratner, M. A. *Quantum Mechanics in Chemistry* (Prentice Hall, Englewood Cliffs, 1993).
25. Poncharal, P., Wang, Z. L., Ugarte, D. & De Heer, W. A. Electrostatic deflections and electromechanical resonances of carbon nanotubes. *Science* **283,** 1513–1516 (1999).
26. Reulet, B. *et al.* Bolometric detection of mechanical bending waves in suspended carbon nanotubes. Preprint cond-mat/9907486 at ⟨http://xxx.lanl.gov⟩ (1999).

Acknowledgements

We thank M. S. Fuhrer and N. S. Wingreen for discussions and advice. This work was supported by the US Department of Energy. E.A. was also partially supported by DARPA.

Correspondence and requests for materials should be addressed to P.M. (e-mail: mceuen@socrates.berkeley.edu).

Gas-phase production and photoelectron spectroscopy of the smallest fullerene, C_{20}

Horst Prinzbach*, Andreas Weiler*, Peter Landenberger*, Fabian Wahl*, Jürgen Wörth*, Lawrence T. Scott†, Marc Gelmont†, Daniela Olevano‡ & Bernd v. Issendorff ‡

* *Institut für Organische Chemie und Biochemie, Albert-Ludwigs-Universität, 79104 Freiburg, Germany*
† *Department of Chemistry, Boston College, Merkert Chemistry Center, Chestnut Hill, Massachussetts 02467-3860, USA*
‡ *Fakultät für Physik, Albert-Ludwigs-Universität, 79104 Freiburg, Germany*

Fullerenes are graphitic cage structures incorporating exactly twelve pentagons[1]. The smallest possible fullerene is thus C_{20}, which consists solely of pentagons. But the extreme curvature and reactivity of this structure have led to doubts about its existence and stability. Although theoretical calculations have identified, besides this cage, a bowl and a monocyclic ring isomer as low-energy members of the C_{20} cluster family[2], only ring isomers of C_{20} have been observed[3–6] so far. Here we show that the cage-structured fullerene C_{20} can be produced from its perhydrogenated form (dodecahedrane $C_{20}H_{20}$) by replacing the hydrogen atoms

with relatively weakly bound bromine atoms, followed by gas-phase debromination. For comparison we have also produced the bowl isomer of C_{20} using the same procedure. We characterize the generated C_{20} clusters using mass-selective anion photoelectron spectroscopy; the observed electron affinities and vibrational structures of these two C_{20} isomers differ significantly from each other, as well as from those of the known monocyclic isomer. We expect that these unique C_{20} species will serve as a benchmark test for further theoretical studies.

The fullerene C_{20}, which may be regarded as the carbon transliteration of "Plato's universe"[7], is shown in Fig. 1 (compound **1**). Unlike C_{60}, the fullerene C_{20} is not formed spontaneously in carbon condensation or cluster annealing processes, as has been demonstrated by extensive ion mobility measurements[6,8]. It seemed to be a safe prediction that cage **1**, if it can be produced at all, would have to be made from a precursor that bore a close structural resemblance to **1**. Furthermore, it would be necessary to produce **1** in the gas phase, as extreme reactivity is expected to result from its strong curvature and flagrant violation of the "isolated pentagon rule"[9]. Even the less-curved fullerene C_{36} is so reactive that it spontaneously oligomerizes in the solid state[10–12].

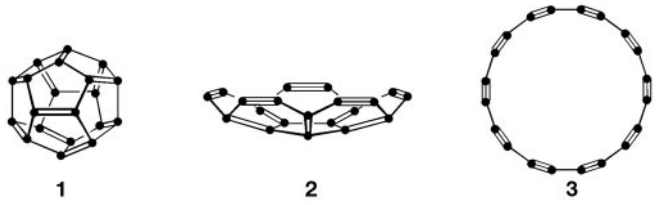

Figure 1 Isomers of C_{20}. **1**, cage; **2**, bowl; **3**, ring.

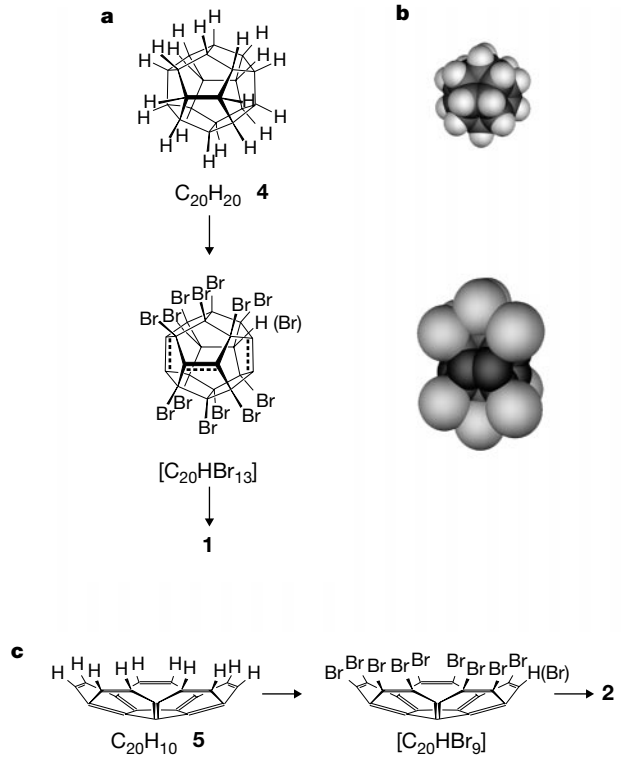

Figure 2 Preparation of precursors for cage **1** and bowl **2**. **a**, Bromination of dodecahedrane **4**. **b,** Space-filling models of $C_{20}H_{20}$ and $[C_{20}HBr_{13}]$ (see text). **c**, Bromination of corannulene **5**.

An obvious starting point for the production of cage **1** is $C_{20}H_{20}$, dodecahedrane (**4** in Fig. 2; refs 13, 14); quantities of this compound that are sufficient for synthetic purposes are now available through the highly optimized "isodrin-pagodane route"[15,16]. To transform **4** into **1**, however, the strongly bound hydrogen atoms must first be replaced by other, more weakly bound atoms, such as chlorine or bromine. Unfortunately, functionalization with sterically less demanding chlorine did not provide a good route to **1**; cation mass-spectroscopic measurements on $C_{20}Cl_{16-20}$ samples did show elimination of chlorine atoms following electron impact ionization, but significant cage fragmentation was also observed[14]. Functionalization of **4** with more weakly bound bromine atoms seemed the way out of this dilemma. There was, however, a significant—and, for a long time, unsolved[14]—synthetic obstacle: the total (or at least near-total) substitution of the small hydrogen atoms by the voluminous bromine atoms failed due to the build-up of excessive molecular strain[17,18]. The way to avoid this obstacle proved to be a 'brute-force' bromination protocol (see Methods), which reproducibly gave a product of average elemental composition $C_{20}HBr_{13}$ (denoted here as $[C_{20}HBr_{13}]$). This product was spectroscopically and chemically identified as primarily a multitude of isomeric $C_{20}H_{0-3}Br_{14-11}$ trienes, which—in spite of their strong deviation from planarity[19] proved oxygen-insensitive (Fig. 2a). During the bromination process, elimination reactions provide relief from the steric overcrowding on the molecular periphery (Fig. 2b). Catalytic reduction of the bromination product back to **4** proved that the cage survived this treatment.

The cation mass spectrum of $[C_{20}HBr_{13}]$ thus prepared (Fig. 3) shows singly and doubly charged C_{20} ions with up to 14 bromine atoms attached. The relative intensities of the $C_{20}H_n^+$ ions (1.0: 0.4: 0.2: 0.1 for n = 0, 1, 2, 3) indicate only minor loss of the residual hydrogen atoms. The high intensity of the C_{20}^+ and C_{20}^{2+} ions and the very low abundance of smaller fragments attests to the remarkable kinetic stability of this C_{20} cluster.

In order to exclude the possibility that cage **1** might have isomerized into the (possibly more stable) bowl **2** during the course of the debromination, we pursued the independent generation of **2**. This was likewise achieved by gas-phase debromination of a $[C_{20}HBr_9]$ precursor prepared by forcing bromination of corannulene **5** (ref. 20; see Fig. 2c and Methods). The 70-eV cation mass spectrum of this material closely resembles that of brominated dodecahedrane, showing C_{20}^+ clusters with up to nine bromine atoms attached (relative intensities of the $C_{20}H_n^+$ ions 1.0: 0.8: 0.8: 0.3 for n = 0, 1, 2, 3).

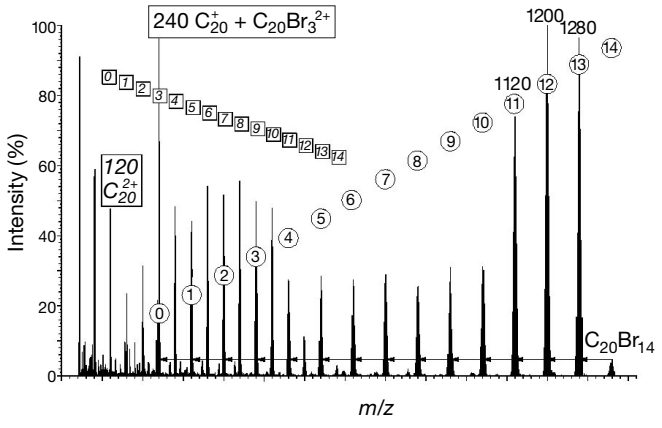

Figure 3 Cation mass spectrum of $[C_{20}HBr_{13}]$; 70-eV electrons were used for ionization. A series of singly charged clusters $C_{20}Br_n^+$ with n = 0–14 (circles), and a similar series of doubly charged clusters $C_{20}Br_n^{2+}$ (squares), can be distinguished. *m/z*, mass-to-charge ratio.

Electron-impact mass spectroscopy alone can neither distinguish between the C_{20} species derived from these two very different brominated hydrocarbons, nor even reveal whether or not they are still different isomers. To establish this, we converted the C_{20} species to their anions, and examined them by photoelectron spectroscopy (PES). In these experiments, a special ion source was used (see Methods) that produces an intense and very stable negative ion beam for several hours from a few milligrams of material. The anion mass spectra obtained for brominated dodecahedrane and brominated corannulene (Fig. 4) resemble those of the cation mass spectra, showing a sequence of brominated C_{20}^- clusters, with the number of attached bromine atoms varying from 13 to 0 in the first case and from 9 to 0 in the second. Again, the high kinetic stability of the C_{20} cluster is manifest.

Photoelectron spectra of mass-selected C_{20}^- clusters obtained from the two brominated precursors, and from graphite in a standard laser evaporation cluster source, are shown in Fig. 5. The spectrum in Fig. 5c is identical to published spectra that have been safely attributed to ring **3** on the basis of ion mobility measurements[6]. The spectra of Fig. 5a and b exhibit notably different features. Both have a reduced electron affinity with respect to ring **3,** and show distinct vibrational patterns. Ring **3** has an electron affinity of 2.44 ± 0.03 eV, and exhibits a vibrational progression of 2,260 ± 100 cm^{-1}. The isomer generated from brominated corannulene has a significantly lower electron affinity of 2.17 ± 0.03 eV, but shows a similar vibrational progression of 2,060 ± 50 cm^{-1}. The isomer generated from brominated dodecahedrane has an electron affinity of 2.25 ± 0.03 eV, and exhibits a vibrational progression of 730 ± 70 cm^{-1}; at 0.27 eV above the first ionization threshold, another progression sets in, this one having a spacing of 260 ± 40 cm^{-1}. The spectra have been measured several times and showed no dependence on the source conditions. Thus, the PES data point to the presence of a single, unique C_{20} isomer in each case. Exact mass selection, however, is crucial; admixture of hydrogenated species $C_{20}H_1^-$ or $C_{20}H_2^-$ led to a blurring of the vibrational structure. The fact that all three anions can be generated selectively, moved over finite periods of time through various parts of the apparatus, separated from other ions, and then photoionized to the neutral carbon allotrope, demonstrates that all three C_{20} clusters, particularly the fullerene C_{20}, have a lifetime of at least the total flight time (0.4 ms).

The measured vibrational pattern of the bowl **2** is in qualitative agreement with predictions (G. Seifert, personal communication). As in ring **3**, the additional electron occupies the lowest antibonding orbital of the triple bonds. Detachment of the electron will thus lead to a high-energy acetylenic stretching mode; the calculations predict frequencies > 2,000 cm^{-1} for such modes[21,22], which agree with the frequencies observed in both cases. For cage **1**, the situation is much more complex; still, the observed 730 cm^{-1} progression is clearly more consistent with that expected for a closed 'polyolefinic' cage (**1**) than with the vibrational progression expected for any other open polycyclic isomer that has acetylenic edges. Unfortunately, it is

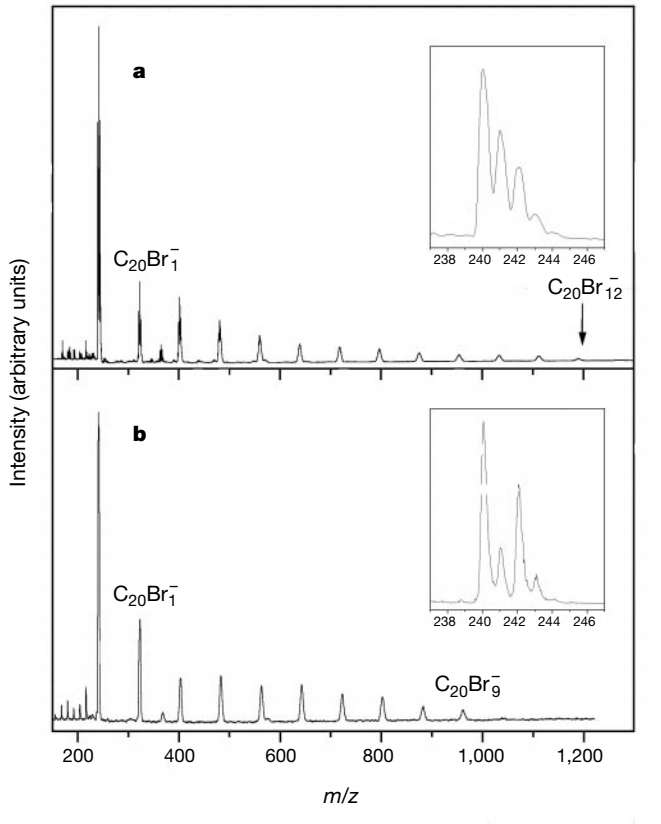

Figure 4 Anion mass spectra of $[C_{20}HBr_{13}]$ (**a**) and $[C_{20}HBr_9]$ (**b**). The molecules have been debrominated and charged by insertion into a gas discharge. In both cases we see a series of $C_{20}Br_n^-$ clusters, with n ranging from 13 to 0 in the upper spectrum (**a**) and from 9 to 0 in the lower spectrum (**b**). Each inset shows a magnification of the C_{20}^- mass peak. Note that due to the natural abundance of the ^{13}C isotope (1.1%), about 18% of the C_{20} intensity appears at mass 241.

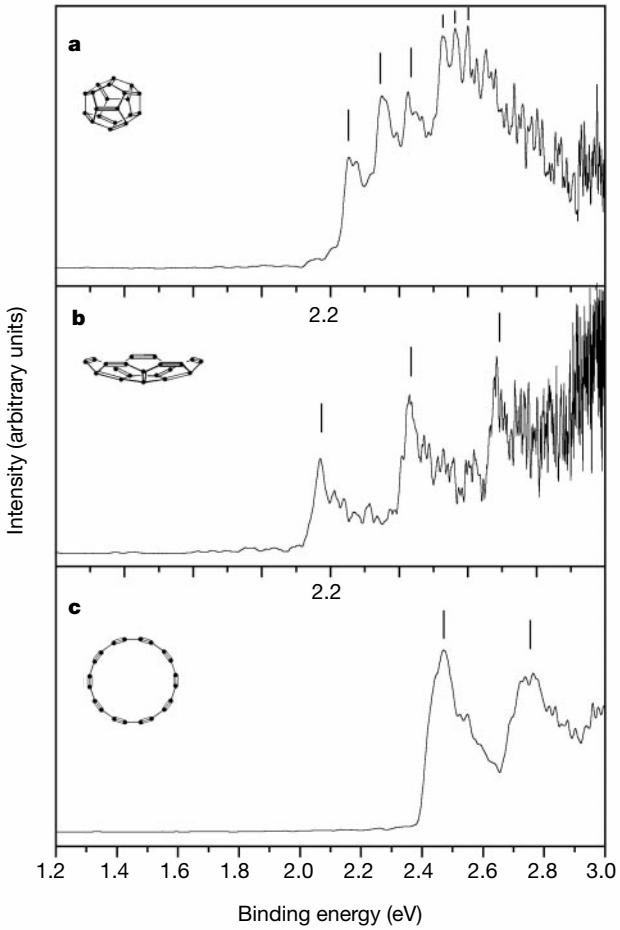

Figure 5 Photoelectron spectra of the mass-selected C_{20}^- clusters. **a**, C_{20}^- produced from $[C_{20}HBr_{13}]$. The wavelength of the detachment laser was 380 nm (3.26 eV). **b**, C_{20}^- produced from brominated corannulene, measured at 380 nm (3.26 eV). **c**, C_{20}^- clusters generated by a standard laser evaporation cluster source, measured at 308 nm (4.03 eV). A KrF excimer laser was used as the evaporation laser, and room-temperature helium as carrier gas.

not yet possible to make definite assignments, in part because the fourfold degeneracy of the highest occupied molecular orbital of the cage is avoided by a Jahn–Teller deformation away from perfect icosahedral symmetry, the nature of which is still disputed[22]. Knowledge of the ground-state symmetry of the neutral cage, however, is indispensable for the prediction of the vibrational modes excited upon electron detachment. We note that there is not even agreement on the relative heats of formation of **1** and **2** in spite of intensive numerical efforts over many years[2]. The photoelectron spectrum of the unique C_{20} species derived from dodecahedrane thus stands as a benchmark test for quantum-mechanical methods. It is hoped that the experimental results reported here will stimulate further theoretical activities.

Until now fullerenes have been produced primarily by carbon condensation processes. The route to cage **1** that we report here is, to our knowledge, the first which makes use of a precursor with a rationally designed carbon core. □

Methods

Bromination procedures

Bromination of **4**: the solution of **4** in dry, deoxygenated bromine was refluxed under visible light irradiation for 3 d in a pressure flask, allowing the generated HBr to leak out. After extraction of the more hydrogen-rich components, the nearly insoluble, deep-red product was sublimed at 300 °C. Bromination of **5**: the solution of **5**, bromine and $FeCl_3$ in 1,1,2,2-tetrachloroethane was refluxed for 24 h.

Mass selection and PES characterization

The precursor substance was immobilized by a drop of toluene within a quartz tube, which was electrically heated to a temperature of 150–250 °C. A pulse of ultrapure helium flushed evaporated material into a copper tube, where a gas discharge was fired by applying a short high-voltage pulse to an isolated pin. The gas discharge fragmented the precursor molecules and negatively charged the products with a very high efficiency. After expansion into the vacuum, the ions entered a reflectron time-of-flight mass spectrometer[23], which could be used either to measure mass spectra of the ions or to insert ions of a given mass into a magnetic bottle photoelectron spectrometer. Here the ions were decelerated and irradiated by a pulsed laser beam. The velocities of the emitted electrons were measured and transformed into a kinetic-energy distribution. The energy resolution of the spectrometer is better than 20 meV for electron kinetic energies below 0.5 eV.

Received 4 October 1999; accepted 6 June 2000.

1. Kroto, H. W. Smaller carbon species in the laboratory and in space. *Int. J. Mass Spectrom. Ions Process.* **138,** 1–15 (1994).
2. van Orden, A. & Saykally, R. J. Small carbon clusters. Spectroscopy, structure, and energetics. *Chem. Rev.* **98,** 2313–2357 (1998).
3. Yang, S. *et al.* UPS of 2–30-atom carbon clusters: Chains and rings. *Chem. Phys. Lett.* **144,** 431–436 (1988).
4. Handschuh, H. *et al.* Stable configurations of carbon clusters: Chains, rings, and fullerenes. *Phys. Rev. Lett.* **74,** 1095–1098 (1995).
5. Wakabayashi, T. *et al.* Photoelectron spectroscopy of C_n^- produced from laser ablated dehydroannulene derivatives having carbon ring size of n = 12, 16, 18, 20 and 24. *J. Chem. Phys.* **107,** 4783–4787 (1997).
6. Von Helden, G. *et al.* Do small fullerenes exist only on the computer? Experimental results on $C_{20}^{+/-}$ and $C_{24}^{+/-}$. *Chem. Phys. Lett.* **204,** 15–22 (1993).
7. Heilbronner, E. & Dunitz, J. D. *Reflections on Symmetry* (VCH, Weinheim, 1993).
8. Von Helden, G., Gotts, N. G. & Bowers, M. T. Experimental evidence for the formation of fullerenes by collisional heating of carbon rings in the gas phase. *Nature* **363,** 60–63 (1993).
9. Kroto, H. W. The stability of the fullerenes C_n with n = 24, 28, 32, 36, 50, 60 and 70. *Nature* **329,** 529–531 (1987).
10. Piskoti, C., Yarger, J. & Zettl, A. C_{36}, a new carbon solid. *Nature* **393,** 771–774 (1998).
11. Fowler, P. W. *et al.* C_{36}, a hexavalent building block for fullerene compounds and solids. *Chem. Phys. Lett.* **300,** 369–378 (1999).
12. Koshio, A., Inakuma, M., Sugai, T. & Shinohara, H. A preparative scale synthesis of C_{36} by high-temperature laser vaporization: Purification and identification of $C_{36}H_6$ and $C_{36}H_6O$. *J. Am. Chem. Soc.* **122,** 398–399 (2000).
13. McEwen, A. B. & Schleyer, P. v. R. In-plane aromaticity and trishomoaromaticity: A computational evaluation. *J. Org. Chem.* **51,** 4357–4368 (1986).
14. Wahl, F., Wörth, J. & Prinzbach, H. The pagodane route to dodecahedranes: An improved approach to the $C_{20}H_{20}$ parent framework; partial and total functionalizations—does C_{20}-fullerene exist? *Angew. Chem. Int. Edn Engl.* **32,** 1722–1726 (1993).
15. Prinzbach, H. & Weber, K. From an insecticide to Plato's Universe—the pagodane route to dodecahedranes: New pathways and new perspectives. *Angew. Chem. Int. Edn Engl.* **33,** 2239–2257 (1994).
16. Bertau, M. *et al.* From pagodanes to dodecahedranes—search for a serviceable access to the parent $C_{20}H_{20}$ hydrocarbon. *Tetrahedron* **53,** 10029–10040 (1997).
17. Cioslowsky, J., Edgington, L. & Stefanov, B. B. Steric overcrowding in perhalogenated cyclohexanes, dodecahedranes, and [60]fulleranes. *J. Am. Chem. Soc.* **17,** 10381–10384 (1995).
18. Beckhaus, H.-D. *et al.* Experimental enthalpies of formation and strain energies for the caged $C_{20}H_{20}$ pagodane and dodecahedrane frameworks. *J. Am. Chem. Soc.* **116,** 11775–11778 (1994); **117,** 8885 (1995).
19. Melder, H.-P. *et al.* Unsaturated dodecahedranes - synthesis of the highly pyramidalized, highly reactive $C_{20}H_{18}$ and $C_{20}H_{16}$ olefins. *Res. Chem. Intermed.* **22,** 667–702 (1996).
20. Scott, L. T. *et al.* Corannulene. A three-step synthesis. *J. Am. Chem. Soc.* **119,** 10963–10968 (1997).
21. Galli, G., Gygi, F. & Golaz, J.-C. Vibrational and electronic properties of neutral and negatively charged C_{20} clusters. *Phys. Rev. B* **57,** 1860–1867 (1998).
22. Duškesas, G. & Larsson, S. Bond lengths and reorganization energies in fullerenes and their ions. *Theor. Chem. Acc.* **97,** 110–118 (1997).
23. Haberland, H., Kornmeier, H., Ludewigt, C., Risch, A. & Schmidt, M. A double/triple time-of-flight mass spectrometer for the study of photoprocesses in clusters, or how to produce cluster ions with different temperatures. *Rev. Sci. Instrum.* **62,** 2621–2625 (1991).

Acknowledgements

We thank J. Leonhardt, G. Leonhardt-Lutterbeck, S. Ruf and C. Warth for technical assistance, and G. Seifert, S. Larsson and R. C. Haddon for discussions. This work was supported by the BASF AG, the Deutsche Forschungsgemeinschaft, the Fonds der Chemischen Industrie, and the US National Science Foundation.

Correspondence and requests for material should be addressed to H.P. (e-mail: horst.prinzbach@orgmail.chemie.uni-freiburg.de).

Chemical characterization of bohrium (element 107)

R. Eichler*†, W. Brüchle‡, R. Dressler§, Ch.E. Düllmann*†, B. Eichler†, H. W. Gäggeler*†, K. E. Gregorich‖, D. C. Hoffman‖¶, S. Hübener#, D. T. Jost†, U. W. Kirbach‖¶, C. A. Laue‖, V. M. Lavanchy*, H. Nitsche‖¶, J. B. Patin‖¶, D. Piguet†, M. Schädel‡, D. A. Shaughnessy‖¶, D. A. Strellis‖, S. Taut#, L. Tobler†, Y. S. Tsyganov, A. Türler*†, A. Vahle#, P. A. Wilk‖¶ & A. B. Yakushev****

** Departement für Chemie und Biochemie, Universität Bern, CH-3012 Bern, Switzerland*
† Labor für Radio- und Umweltchemie, Paul Scherrer Institut, CH-5232 Villigen, Switzerland
‡ Gesellschaft für Schwerionenforschung, D-64291 Darmstadt, Germany
§ Institut für Analytische Chemie, Technische Universität Dresden, D-01062 Dresden, Germany
‖ Nuclear Science Division, Lawrence Berkeley National Laboratory, California 94720, USA
¶ Department of Chemistry, University of California at Berkeley, California 94720, USA
 # Institut für Radiochemie, Forschungszentrum Rossendorf, D-01314 Dresden, Germany
*** Flerov Laboratory of Nuclear Reactions, Joint Institute for Nuclear Research, 141980 Dubna, Russia*

The arrangement of the chemical elements in the periodic table highlights resemblances in chemical properties, which reflect the elements' electronic structure. For the heaviest elements, however, deviations in the periodicity of chemical properties are expected[1–3]: electrons in orbitals with a high probability density near the nucleus are accelerated by the large nuclear charges to relativistic velocities, which increase their binding energies and cause orbital contraction. This leads to more efficient screening of the nuclear charge and corresponding destabilization of the outer d and f orbitals: it is these changes that can give rise to unexpected chemical properties. The synthesis of increasingly heavy elements[4–6], now including that of elements 114, 116 and 118, allows the investigation of this effect, provided sufficiently long-lived isotopes for chemical characterization are available[7]. In the case of elements 104 and 105, for example, relativistic effects interrupt characteristic trends in the chemical properties of the elements constituting the corresponding columns of the periodic table[8], whereas element 106 behaves in accordance with the